Available online at www.sciencedirect.com
SCIENCE DIRECT
Polymer 46 (2005) 9423–9433
polymer
www.elsevier.com/locate/polymer

Use of molecular dynamics to investigate polymer melt–metal wall interactions

Uğursoy Olgun*, Dilhan M. Kalyon

Department of Chemical, Biomedical and Material Engineering, Stevens Institute of Technology, Castle Point Station, Hoboken, NJ 07030, USA

Received 6 June 2005; accepted 14 July 2005
Available online 10 August 2005

Abstract

The classical boundary condition of fluid dynamics, i.e. the no-slip condition is violated during the flow of various complex fluids including polymer melts and polymeric suspensions. It is recognized that the dynamics of the behavior of the macromolecules at the wall, their adsorption, and disentanglement from each other and from the wall all play significant roles during shearing and flow. During wall slip it is not clear whether the macromolecules detach from the wall (adhesive failure of the slip condition) or whether the macromolecules remain tethered to the wall but disentangle from the neighboring macromolecules (cohesive failure). In this study, we seek to shed light to the basic mechanisms of the wall slip of polymers by focusing on the dynamics of the polymer behavior at the wall for three polymers, two of which exhibit significant strong wall slip, high density polyethylene (HDPE) and poly(dimethylsiloxane) (PDMS), and one which does not exhibit wall slip under typical extrusion conditions, i.e. a block copolymer BAMO/AMMO, (crystalline blocks of poly(3,3-bis(azidomethyl)-oxetane), BAMO, and amorphous blocks of poly(3-azidomethyl)-3-methyl-oxetane, AMMO). The cohesive energy densities of the three polymers were found to be in the same range, with the cohesive energy density of BAMO/AMMO being slightly higher than those of the other two. The molecular dynamics based cohesive energy density values compared well with calculations based on the determination of the group molar attraction constants. On the other hand, the energy of adhesion value exhibited by the copolymer BAMO/AMMO/iron oxide is significantly higher than the energy of adhesion values for the iron oxide/PDMS and iron oxide/HDPE systems. Considering that over the same broad range of shear stresses the block copolymer BAMO/AMMO does not exhibit wall slip and the other two polymers HDPE and PDMS do, these findings suggest that at least for these three polymers wall slip is more likely to occur on the basis of an adhesive failure mechanism.

Keywords: Polymer-metal adhesion; Molecular dynamics; Polymer melt

1. Introduction

Ab initio or molecular dynamics (MD) based simulations of macromolecules have great technological importance since they often provide a detailed understanding of many flow processes, which especially occur at solid interfaces. A wide variety of materials and interfaces have been simulated so far. For example, the molecular dynamics, MD, simulation techniques were employed by Abloo et al. in their investigation of the interfaces between the polymeric electrolytes and the electrodes [1]. For the V_2O_5 electrode and a polyethylene oxide electrolyte targeted for the Li-ion battery, they have shown that the dynamics of the motion at the solid/polymer interface is controlled by interactions between the ether oxygen of the PEO polymer and the V=O bonds of the metal. In another application, the heat of mixing values of various blends of polymers were investigated to determine if pairs of polyethylene oxide, polypropylene and polyacrylic acid were miscible or not [2]. In yet another application, Karthigeyan and Myerson have investigated the nucleation and the crystallization of isotactic polypropylene in the absence and presence of a nucleating agent using molecular dynamics simulations [3]. The results were found to be in good agreement with the experimental observations. The interactions of hydrocarbon clusters representing polyethylene with Al, Cu, and Zn were studied using an ab initio atomic cluster model and stronger

* Corresponding author. Address: Department of Chemistry, Sakarya University, Mithatpaşa, Sakarya 54100, Turkey. Tel.: +90 264 346 0378; fax: +90 264 346 0371.
E-mail address: ugursoyolgun@yahoo.com (U. Olgun).

0032-3861/$ - see front matter © 2005 Elsevier Ltd. All rights reserved.
doi:10.1016/j.polymer.2005.07.042

interaction (greater potential energy) was observed for hydrocarbon–Al interface in comparison to the interactions of the hydrocarbon cluster with the other metals [4].

Molecular dynamics calculations have also revealed that the variations in the solid-wall and fluid interaction affect the distribution of the density of the fluid adjacent to the wall, leading to changes in the viscosity of the fluid [5]. The motion of nanoparticles confined in nanochannels has also been investigated and the motion of the particle at the wall is observed to be a slip-stick flow as affected by the interaction parameter between the wall and the fluid [5].

The present investigation was initiated upon the observation that the violation of the no-slip boundary condition during the flow and deformation of polymer melts is affected by the nature of the interface formed between the metal and polymer [6–12]. Furthermore, we have recently determined that given a wall material of construction, some polymers exhibit a catastrophic failure of the no-slip condition, while some others exhibit the no-slip condition over a broad range of shear stresses and shear rates during flow[13]. In this study, it was determined that PDMS and HDPE do exhibit strong wall slip in simple shear flows (upon the wall shear stress reaching the critical wall shear stress values of 0.2 and 0.07 MPa, respectively [13]), whereas BAMO/AMMO block copolymer does not exhibit a catastrophic failure of the no-slip condition at the wall of the rheometer with stainless steel fixtures over a broad range of shear stress values [13]. Thus, a good starting point for understanding of the fundamentals of the interaction between the metal surface and the polymer melt appeared to be the carrying out of molecular dynamics calculations of the same polymers with a typical material of construction for the wall (oxidized iron surface).

The BAMO/AMMO is a recently developed elastomer and its chemical structure is given below along with the other polymers of the study:

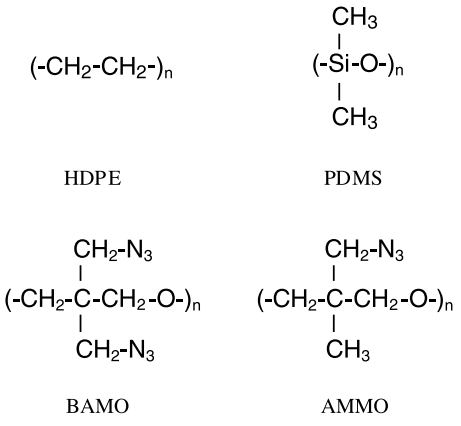

The BAMO fraction is crystalline and the AMMO fraction is amorphous, thus generating a thermo plastic elastomer with BAMO hard blocks and AMMO soft blocks.

2. Molecular dynamics (MD)

For the molecular dynamics calculations, a commercially-available source code, Cerius[2] of Molecular Simulation Incorporated of San Diego, California was used [14]. Macromolecules were generated using the Amorphous Builder module with periodic boundary condition and then relaxed using energy minimization procedures. Both constant *NVE* (constant volume, energy and number of atoms) dynamics and constant *NPT* (constant pressure, temperature and number of atoms) simulations were performed. The cell size was taken to be more than twice the van der Waals radius in order to avoid the periodic nature of the model fluid [3]. The Dreiding force field (a purely diagonal force field with harmonic valance terms and a cosine-Fourier expansion torsion term) was used for the calculations [15]. The van der Waals interactions were calculated from the Lennard–Jones potential. Electrostatic interactions were described by atomic monopoles and distance-dependent Coulombic term. Hydrogen bonding is calculated by an explicit Lennard–Jones 12–10 potential. During the simulations, the following specific procedure was employed.

2.1. MD simulation of polymer melts

1. Following Karthigeyan and Myerson, the typical model for the simulation employed the use of four polymer chains (the number of backbone atoms in each chain were 90 for HDPE, 90 for PDMS and 80 for BAMO/AMMO), which were all in their random configurations [3]. The Amorphous Builder module of the software was employed to represent the macromolecules in molten state [14]. The four chains were taken to represent the bulk state of the polymer melt in conjunction with a 3D periodic system.
2. In the 3D periodic system, a cube of typical side length of 30–40 Å was constructed to contain the four chains at the desired density value (initially low). A bump-checking algorithm was used to control how close the nonbonded atoms of the molecules could come together. In this procedure, the allowable distances pertain to the van der Waals radii of the two atoms, r_0, multiplied by the van der Walls scale, R [14]. A value of $R=0.89$ is taken for the maximum value of the distance at which the potential energy U becomes equal to zero, i.e.:

$$U(0.89r_0) = 0 \tag{1}$$

   This is the distance at which the Lennard–Jones 12–6 potential becomes repulsive [14]. A default value of $R=0.3$ was used in our simulations.
3. The stable conformations of the macromolecules (for which the net force on each atom vanishes) were determined by the adjustment of the atomic coordinates

to minimize the potential energy of the system. During this minimization the dimensions of the simulation box were kept constant. Initially the density of the system was kept relatively low (0.3–0.5 g/cm^3).

4. The potential energy of the system was provided as an empirically-fitted expression designated as the force field which employs a combination of internal coordinates, terms containing the bond distances, bond angles, torsions, etc. for the description of the interactions between bonded atoms and to describe the interactions between the nonbonded atoms dependent on the distance of separation, i.e. the van der Waals or dispersion, and electrostatic and hydrogen bonding interactions between the atoms. For the minimization of the potential energy, a number of options were available. We have selected to work with the generic force field Dreiding [15]. In Dreiding the valance interactions are made up of the bond stretch, bond angle bend, dihedral angle torsion and the inversion terms [15].
5. For the minimization of the potential energy function, three minimization algorithms were available, i.e. the Steepest Descent, the Conjugate Gradient and the Newton–Raphson methods [14]. These three methods were used interchangeably.
6. The final minimized potential energy conformations of the chains constituted the starting point for the determination of the equilibrium structure using the molecular dynamic method. Various options were available and we have selected to work with constant cell content, constant volume and constant energy (*NVE*) dynamics [14]. The equilibrium configuration of the chains refers to a homogeneous distribution of the chains in the simulation box at a target temperature of 400 K.
7. For the integrator, the Verlet leapfrog was used [14].
8. At this point, the density of the system was still at the lowest value assigned at the beginning of the simulation run. The correct density of the system was achieved by running a constant pressure and constant temperature (*NPT*) simulation [14]. During this part of the simulation the vectors of the simulation cell were allowed to change and the pressure was adjusted by altering the volume of the simulation box. During the simulation, i.e. the solution of the Newton's equation, the temperature was maintained at 440 K for polyethylene, 454 K for PDMS and 500 K for BAMO/AMMO by coupling to an external bath, following Berendsen et al. (this is referred to as T-damping in Cerius^2) [16]. The pressure was set at 1 GPa for the simulation.
9. The cohesive energy density for each polymer was determined by first minimization of the potential energy of the macromolecules at the desired density of the simulation box and the determination of the minimum potential energy value at this density achieved at the end of step 8. This is followed by a systematic increase of the cell dimensions until the macromolecules are so apart that there are no intermolecular forces acting on the atoms. Upon reaching the asymptotic energy associated with the systematically augmented volume of the simulation cell, the difference between this energy state (E_2) at which the macromolecules can no longer feel each other and the potential energy (E_1) associated with the correct melt density of the macromolecule is determined and then divided with the molar volume (V) prior to augmentation. The cohesive energy of the macromolecule was then defined as the increase in energy per mole of the macromolecule if all of the intermolecular forces were eliminated. The cohesive energy densities, E_{CED}, shown in Table 1 were calculated according to the Eq. (2) given below.

$$E_{CED} = \left(\frac{E_2 - E_1}{V}\right) \quad (2)$$

10. The final conformations of the macromolecules were then stored in a trajectory file for the calculation of the work of adhesion, the procedure of which is described next.

2.2. MD simulation of polymer melt–iron interface

The starting point of analysis was the amorphous polymer structures. Polymer–iron interfaces were then built in a second step and equilibrated. Adhesion characteristics of HDPE, PDMS and BAMO/AMMO to iron surface were investigated by the following approach:

1. Here, we have considered oxidized surfaces of Fe, i.e. the Fe_2O_3. The unit cell structure of the Fe_2O_3 was available and the morphology calculations were carried out with the Morphology module of Cerius^2 [14]. This technique followed the Bravais Friedel Donnay Harker (BFDH) method which is based on the approximation of the crystal morphology using a set of geometrical rules based on the available lattice parameters (the dimensions of the unit cell, the angles between faces of the unit cell, the space group) and the atomic coordinates [17]. For the case of the Fe_2O_3, the largest face of the crystal was the 012 surface and therefore, it was used as the surface

Table 1
Calculated cohesive energy values of BAMO/AMMO, HDPE, and PDMS

Polymer	Simulation density (g/cm^3)	Coulomb energy (cal/cm^3)	VDW energy (cal/cm^3)	Cohesive energy (cal/cm^3)
BAMO/AMMO	1.2	−43	−38	−81
HDPE	0.9	−67	−2	−69
PDMS	1.2	−58	−3	−61

Table 2
Calculated adhesive energy values of BAMO/AMMO, HDPE, and PDMS melts with the iron wall

Polymer–Fe interface	Simulation density[a] (g/cm^3)	Coulomb energy (cal/cm^3)	VDW energy (cal/cm^3)	Adhesive energy (cal/cm^3)
BAMO/AMMO–Fe	2.1 (1.2)	−132	−7	−140[b]
HDPE–Fe	1.9 (0.9)	−47	−13	−60
PDMS–Fe	1.9 (1.1)	−60	−8	−68

[a] The density of each polymer without the Fe wall is given in parenthesis.
[b] Hydrogen bonding contribution of −1 cal/cm^3 was also included.

against which the macromolecules came into contact during the simulation.

2. Using the Surface Builder module of Cerius^2 and defining a slab thickness of 8 Å for the wall thickness, the metal surface was prepared employing the 012 plane. An additional hydrogen atoms was incorporated to the surface to neutralize the charge resulting from the surface formation since the oxygen cannot be packed at the surface as effectively as in the bulk of the metal. During this step the bond distances between selected atoms at the surface of the metal were adjusted. The same task could be accomplished by using the minimization of the potential energy at the surface. Upon completion of energy minimization, the surface structure was converted into a nonperiodic super structure for use in the crystal surface building step.
3. Using the Crystal Builder facility of Cerius^2 the crystals of the metal slabs to be used in the simulation box for the work of adhesion calculation were built in one simulation cell. However, the dimensions of the simulation cell used here needs to be matched with the dimensions of the simulation cell used earlier for the work of cohesion calculations. This was done using the Visualizer facility of the Crystal Builder to generate a super lattice structure of the wall slabs to enable the fitting of the dimensions of the earlier simulated polymers with those of the wall slabs. This was carried out by increasing the number of cells used for the simulation and then by removing the partitions between the cells. The surface area selected for the metal consisted of 4*a* times 4*b* (where *a* and *b* are the unit cell dimensions for Fe_2O_3) for the simulation of HDPE and 5*a* times 5*b* for PDMS and BAMO/AMMO.
4. The charge equilibration approach was employed to determine the atomic electronegativities and the charge distribution for the wall slabs [14]. The same was done for the polymers also. Furthermore, prior to integrating the macromolecules into the simulation box (prepared with the metal wall slabs placed as its boundaries), the macromolecules were converted into nonperiodic superstructures.
5. The macromolecules were dragged into the simulation box with the metal wall slabs and the *c* dimension of the box was adjusted so that the macromolecules were equally distant from the two walls and there was no diffusion through the wall.
6. Using *NPT* dynamics (constant pressure, temperature and number of atoms) the volume of the simulation box was progressively decreased using a 0.001 ps time interval for the calculations for a total duration of 20 ps. The pressure was held at 1 GPa. It was determined that the temperature varied during the simulation and in general was at a greater value in comparison to the targeted temperature for each of the three polymers. However, additional typical *NVE* (constant number of moles, volume, and energy) calculations, which were carried out for longer durations, allowed achieving the targeted temperature.
7. Considering that the system is periodic during the molecular mechanics and molecular dynamics calculations, the Ewald technique [18,19] was used for the computation of the nonbond energies as suggested by Myerson et al. [3].
8. The potential energy of the system was minimized and the value of the minimum potential energy was determined. For the determination of adhesion energy, two consecutive steps were followed. In the first step, the wall slabs were removed from the simulation box and the corresponding

Table 3
Calculated solubility parameters of BAMO/AMMO, HDPE, and PDMS

Polymer	Simulation density (g/cm^3)	Cohesive energy (E_{CED}) (cal/cm^3)	Solubility parameter $\delta=(\lvert E_{CED}\rvert)^{1/2}$ (cal/cm^3)$^{1/2}$	Solubility parameter $\delta=\rho\sum G/M$ (cal/cm^3)$^{1/2}$
BAMO/AMMO	1.2	−81	9.0	9.3
HDPE	0.9	−69	8.3	8.5
PDMS	1.2	−61	7.8	7.6

Table 4
Selected bond distances of BAMO/AMMO, HDPE, and PDMS at the iron wall

Polymer–Fe interface bonds	Average bond distances in Å (number of bonds)		
	BAMO/AMMO	HDPE	PDMS
CH_2–N_3···Fe	2.673(5)	–	–
CH_2–N_3···HO–Fe	2.699(14)	–	–
C–CH_3···OH–Fe	2.849(7)	–	–
N_3–CH_2···OH–Fe	2.812(7)	–	–
CH_2–CH_2···OH–Fe	–	2.798(14)	–
Si–CH_3···OH–Fe	–	–	2.786(21)
Number of contact (<3 Å)	33	14	21

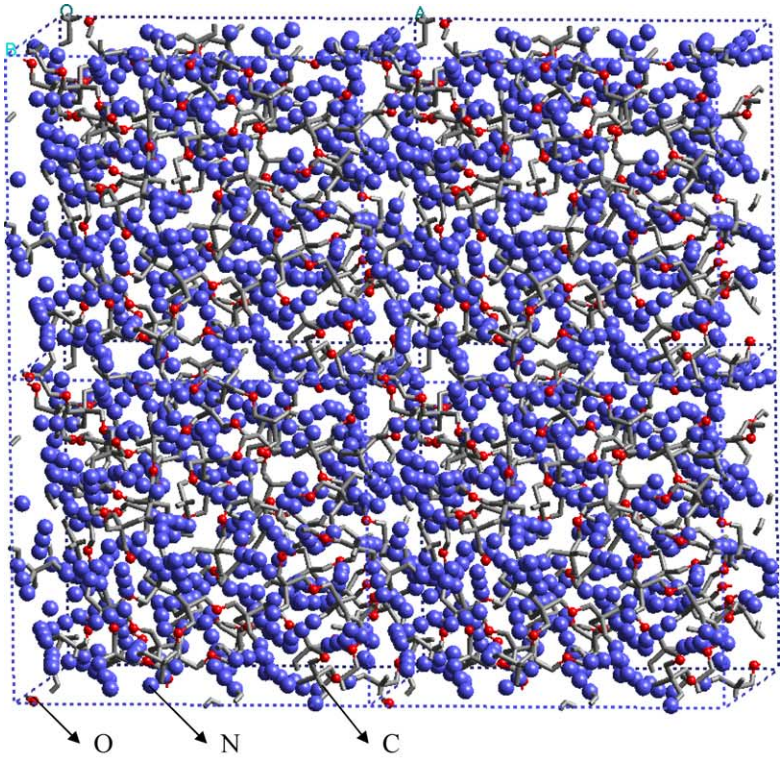

(a) BAMO/AMMO

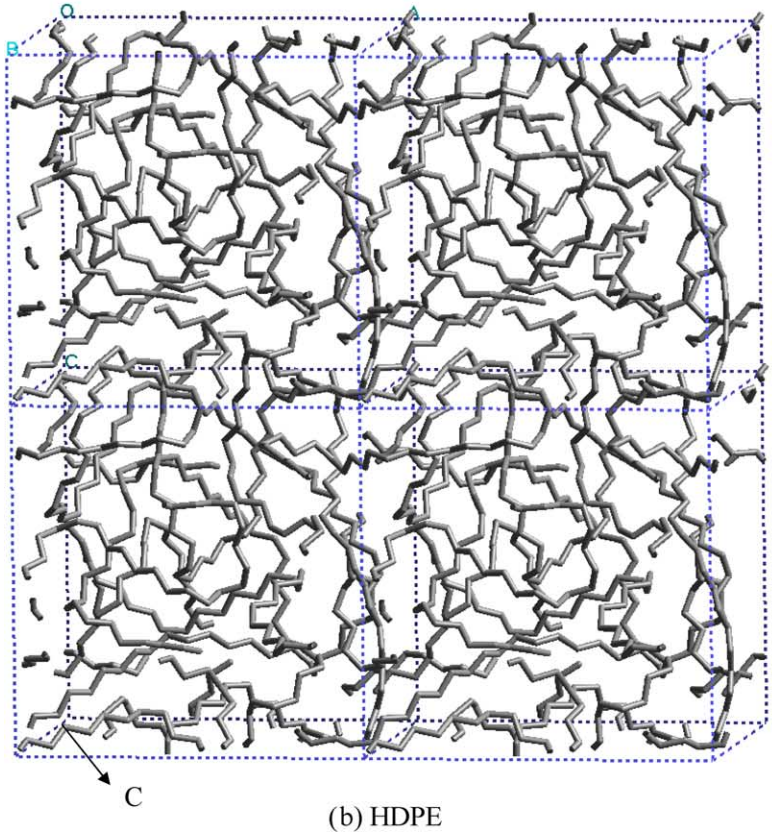

(b) HDPE

Fig. 1. Simulated BAMO/AMMO, HDPE, and PDMS polymer melts and their interfaces with the iron surface.

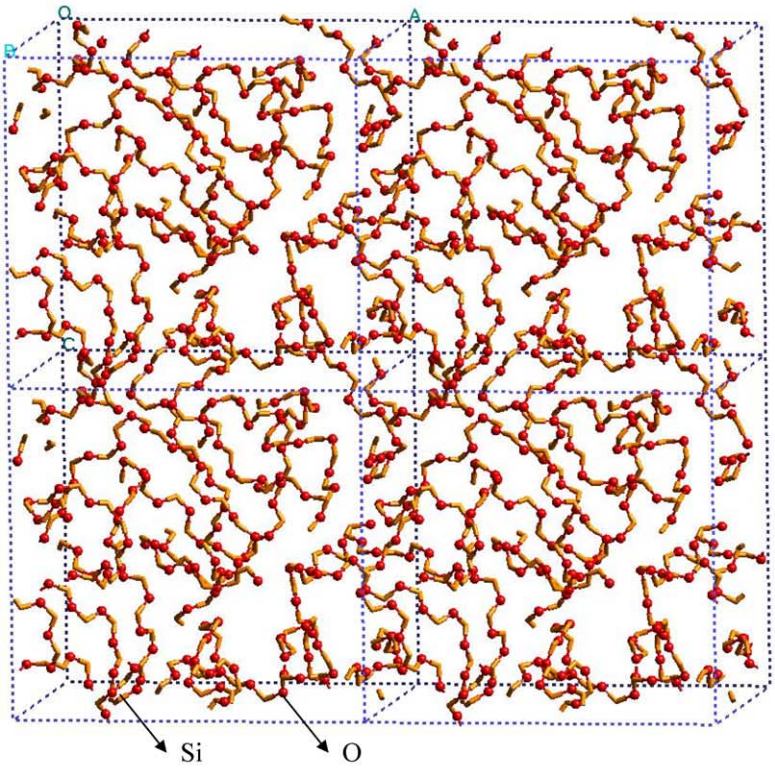

(c) PDMS

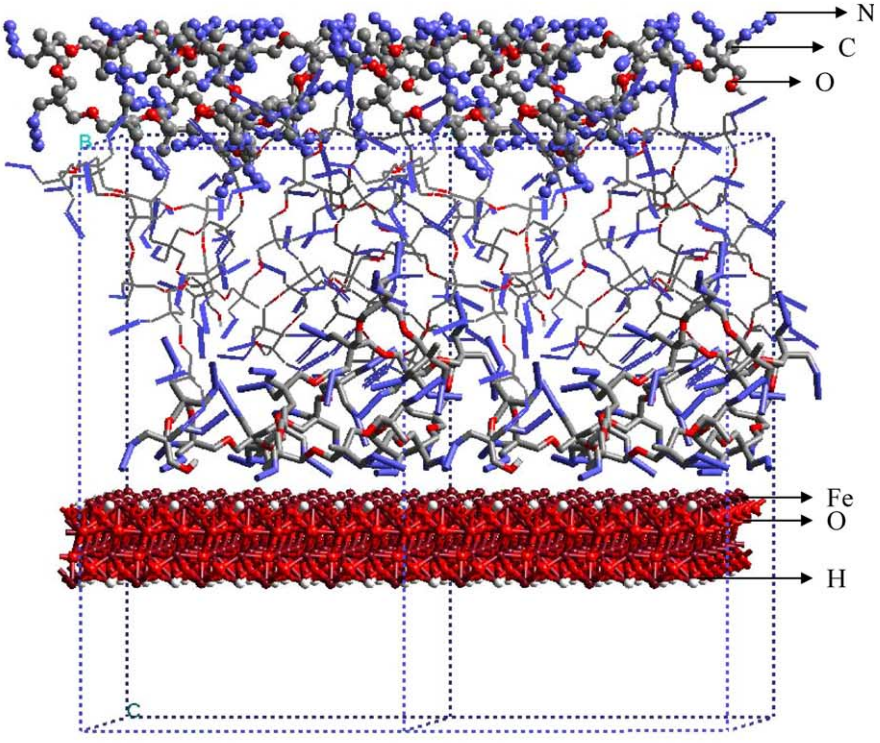

(d) BAMO/AMMO-Fe

Fig. 1 (*continued*)

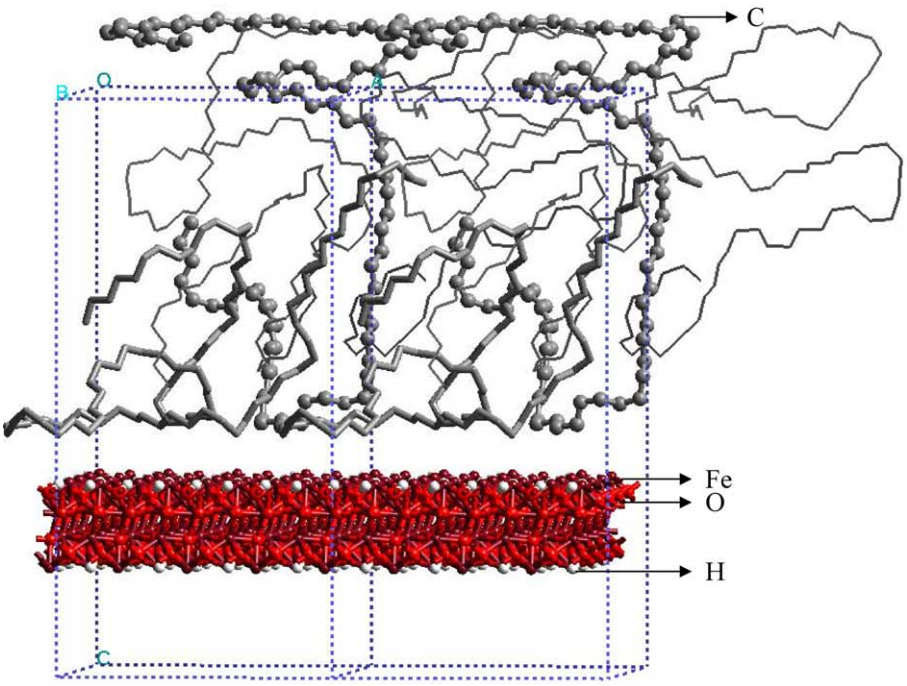

(e) HDPE-Fe

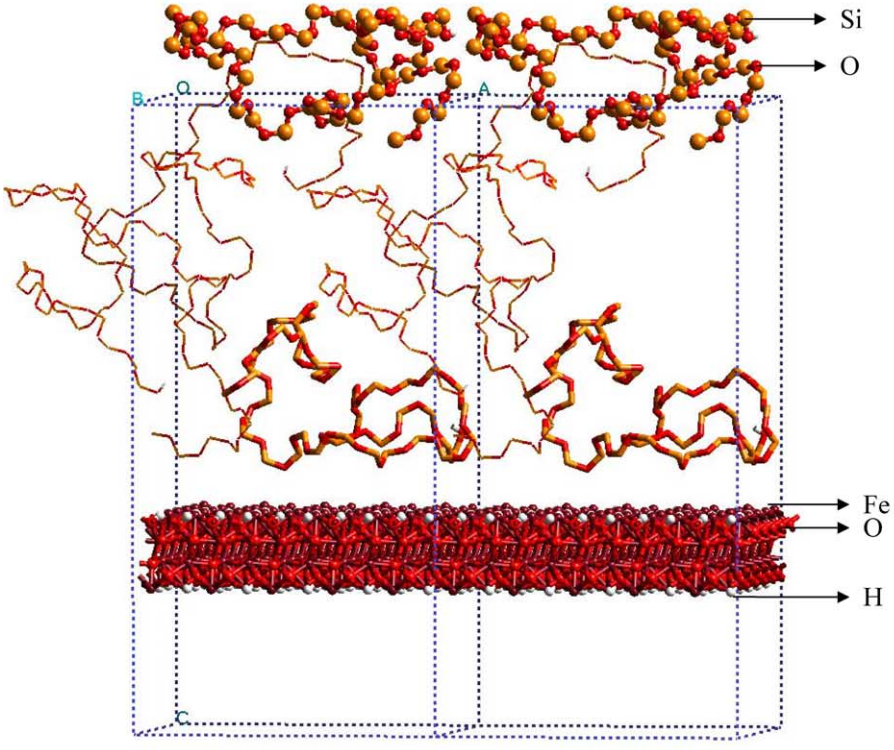

(f) PDMS-Fe

Fig. 1 (*continued*)

potential energy was determined. In the second step, the wall was kept and the polymer chains were removed from the simulation box and the corresponding potential energy value was determined. The energy of adhesion, E_A, was determined according to the Eq. (3) by dividing the difference between the potential energy minimum of the simulation box containing both the polymer chains and the wall slabs, E_{12}, with the sum of the potential energies of the wall slabs, E_1, and the polymer chains, E_2, (calculated without the presence of each other in the simulation box)

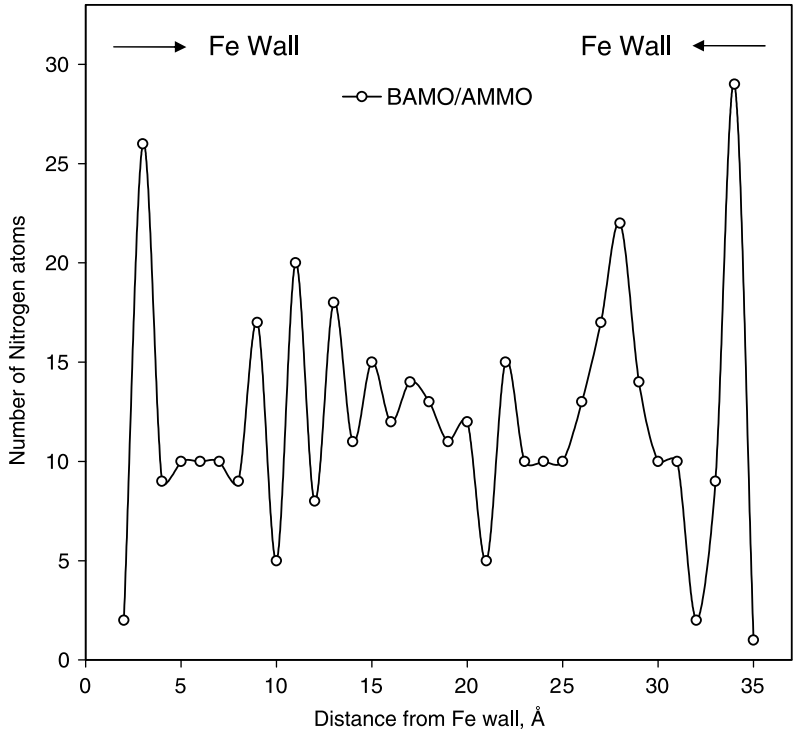

Fig. 2. Distribution of nitrogen atoms of BAMO/AMMO as a function of distance between the two iron walls.

with the molar volume, V. Calculated adhesion energies are given in Table 2.

$$E_A = \frac{E_{12} - (E_1 + E_2)}{V} \tag{3}$$

3. Results and discussion

The typical configurations of macromolecules during the cohesive and adhesive energy calculations are shown in Fig. 1. The number of segments of chains found in the vicinity of the metal wall is greater for the elastomer BAMO/AMMO in comparison to PDMS and HDPE. There also seem to be significant differences in the alignment and configurations of the macromolecules for the three polymers.

The results of the calculations are summarized in Tables 1 and 2. The tables contain the simulation density of polymer melts, the Coulomb energy, the van der Waals energy, hydrogen bonding energy and the cohesive energy for the pure polymer and the adhesive energy for the metal–polymer interactions. The cohesive energy is made up of three parts including the Coulomb, van der Waals and hydrogen bonding. Among these, the Coulomb energy is the highest contributor to the development of the cohesive energy values of the three polymers. However, for the BAMO/AMMO the van der Waals energy is also relatively significant and about one order of magnitude greater than the values of van der Waals energy for the other two polymers. Hydrogen bonding is negligible for all three polymers in the determination of cohesive energy. The cohesive energy density is related to Hildebrand's solubility parameter, through the equation:

$$\delta = (|E_{CED}|)^{1/2} \tag{4}$$

Table 3 shows the solubility coefficient values for the three polymers as determined from the cohesive energy density values obtained from the simulations using Eq. (4). These results were compared with those determined from the group molar attraction constants of the groups, which constitute each polymer and the Eq. (5):

$$\delta = \frac{\rho \sum G}{M} \tag{5}$$

Where ρ, G and M represents the density, the molar attraction constant and the mer molecular weight, respectively [20]. Group molar attraction constants at 25 °C were calculated from the measurement of heat of evaporation by Small [21]. The G values were not available for the azido group of BAMO/AMMO and the molar attraction constant of the azido group was assumed as 400 (based on the G values of CN, 410 and NO_2, 440). Overall, there is good agreement between the two separate sets of values for all three polymers, suggesting the adequacy of the simulation methodologies. Overall, the cohesive energy density of BAMO/AMMO is slightly greater than the cohesive energy densities of the PDMS and HDPE as given in Table 1, however, the differences are not that significant.

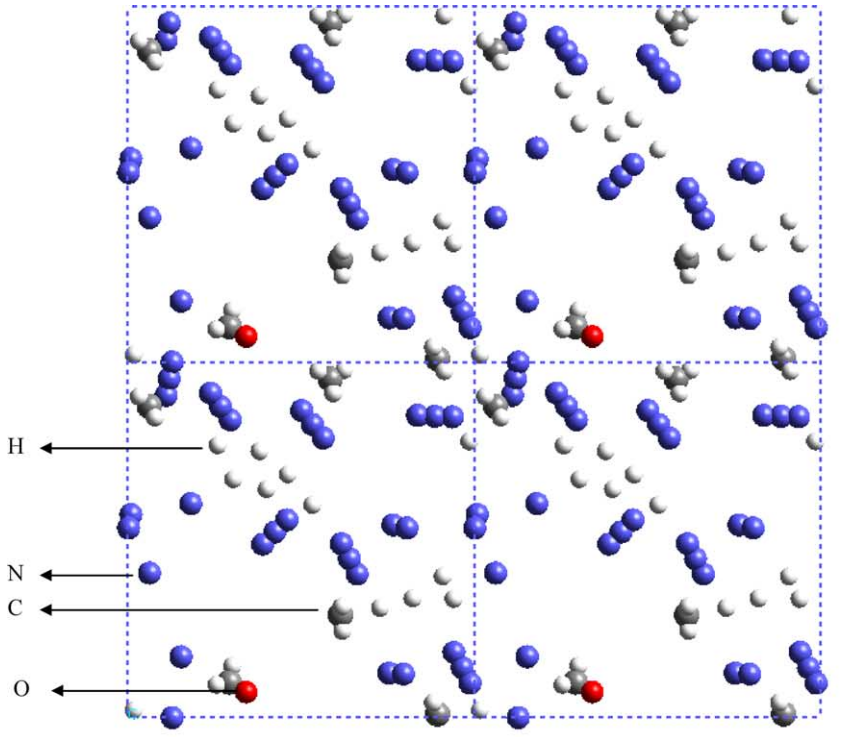

(a) BAMO/AMMO

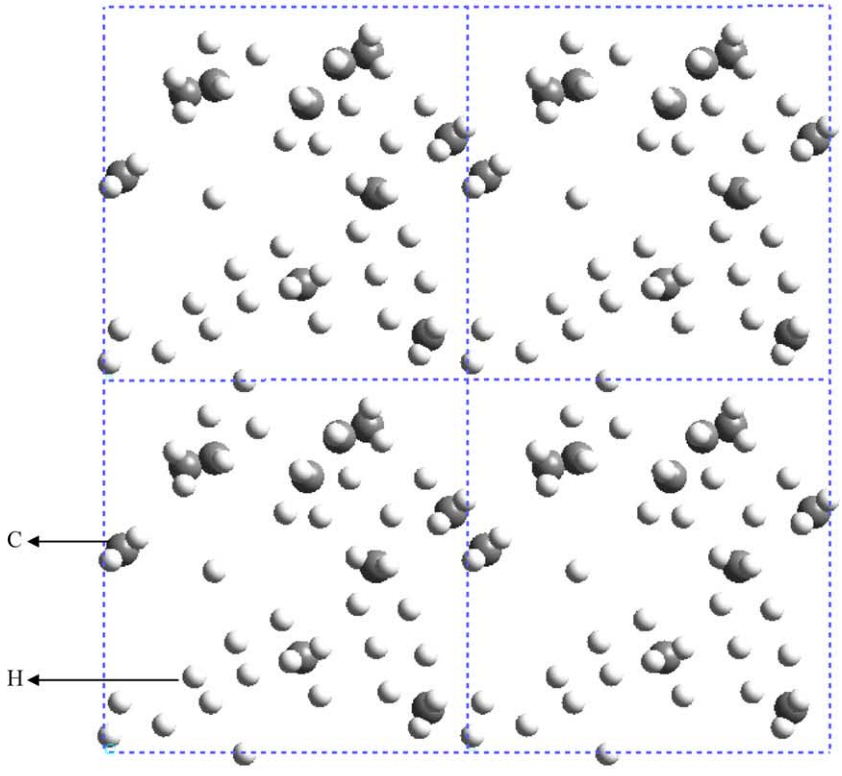

(b) HDPE

Fig. 3. Interface atoms of BAMO/AMMO, HDPE, and PDMS melts at 2 Å above the iron wall (1 Å depth slices).

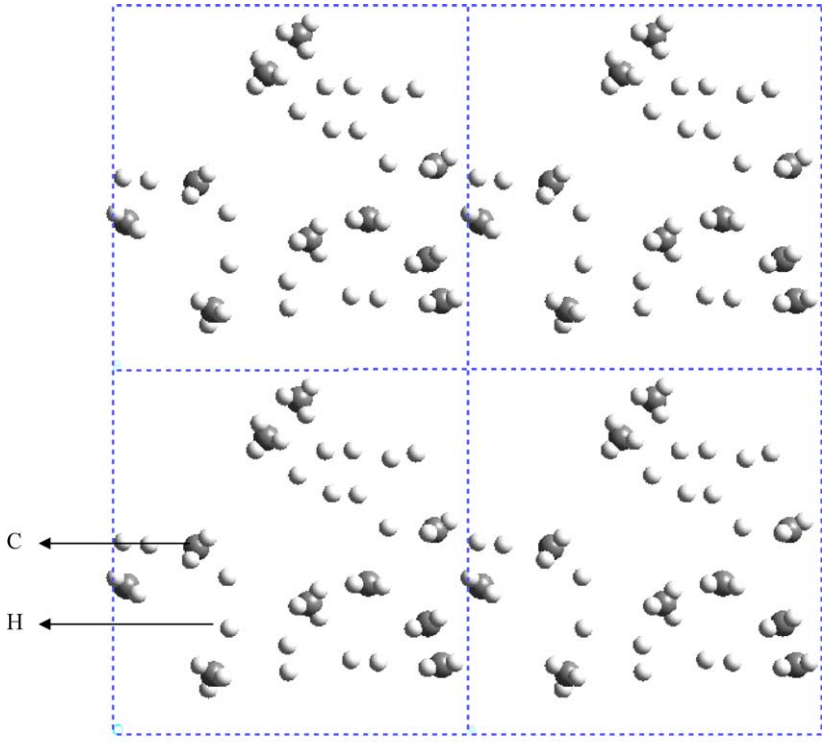

(c) PDMS

Fig. 3 (*continued*)

The cohesive energy density values calculated here suggest that there are no significant differences in the affinities of the macromolecules of the three melts which are tethered to the wall to detach from the next layer of macromolecules, if the cohesive energy density is taken to be indicative of the energy necessary to disentangle the macromolecules tethered to the wall from the rest.

On the other hand, the energy necessary to separate the segments of the polymer from the oxidized iron surface (adhesive energy value) is significantly greater for the BAMO/AMMO in comparison to the other two polymers. The adhesive energy value of BAMO/AMMO is greater than twice that of HDPE and PDMS. The biggest contribution to adhesive energy stems from the Coulomb energy, which should be associated with the electronegativity and the resulting charge distribution arising from the presence of the nitrogen atoms in BAMO/AMMO. The number of nitrogen atoms at the BAMO/AMMO-iron wall interface was greater than the number of nitrogen in the polymer bulk as shown in Fig. 2. This is due to the strong electrostatic interactions between the negatively charged azido groups of BAMO/AMMO and the positively charged Fe^{3+} and $H^{\delta+}$ of metal wall. Selected bond distances at different polymer–iron interfaces are listed in Table 4. These findings clearly indicate a greater number of close contacts with small bond distances between BAMO/AMMO elastomer and the wall. The atomistic structures of polymers at 2 Å above the metal wall are demonstrated as 1 Å depth slices in Fig. 3. Unlike BAMO/AMMO elastomer, HDPE and PDMS showed similar compositions with a large number of hydrogen atoms at the interface. On the other hand, BAMO/AMMO–iron interface includes significant number of nitrogen atoms and yields a greater density in short distances from the metal wall. Fig. 4 shows the segment density versus the distance from the metal wall behavior of the three polymers. The increased density at the wall is indicative of the greater affinity to adsorption and immobilization of polymer chains on the wall. All three polymers were coiled randomly at the beginning of simulations and clear orientations could be observed for the final configurations of HDPE and BAMO/AMMO macromolecules.

The greater adhesion energy of BAMO/AMMO for the metal surface should be related to the observed unusual stickiness of BAMO/AMMO with the metal surface, which made the loading of its melt to the heated reservoir of the rheometers used very difficult. This type of stickiness was not observed for the other two polymer melts. The greater energy of adhesion of BAMO/AMMO should also play a significant role in the observed no-slip condition at the wall for BAMO/AMMO [13]. This flow behavior of BAMO/AMMO at the wall was markedly different than the behavior of the other two polymer melts (HDPE and PDMS) which both exhibited strong slip, i.e. the catastrophic failure of the no-slip condition at the wall [13].

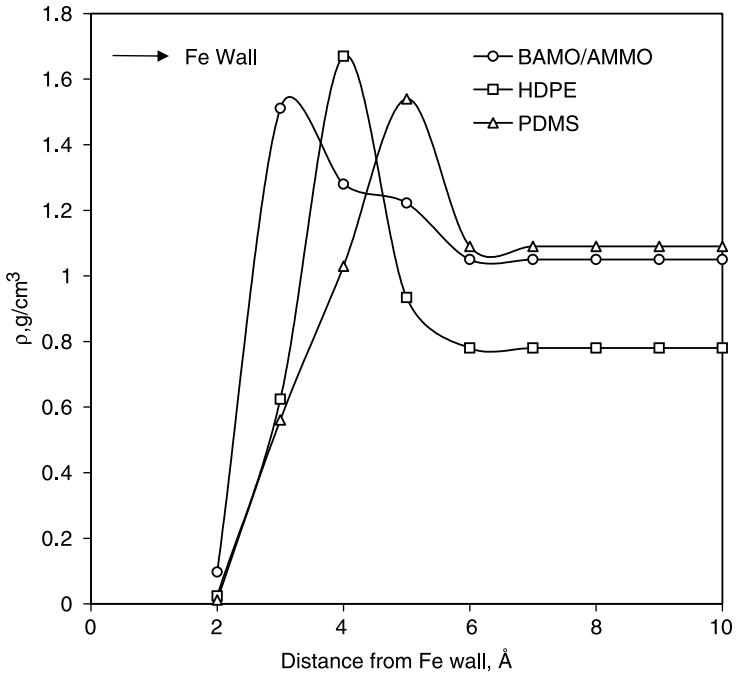

Fig. 4. Density distribution of BAMO/AMMO, HDPE, and PDMS melts as a function of distance from the iron wall.

The extrudates of the three polymers upon exit from capillary rheometry were also very different as demonstrated by Kalyon and Gevgilili [13]. The extrudates of BAMO/AMMO were smooth and did not exhibit any gross surface irregularities such as melt fracture and shark skin formation. On the other hand, the extrudates of PDMS and HDPE exhibited gross surface irregularities, which were onset at critical values of the wall shear stress, which coincided with the shear stress at which the no-slip condition catastrophically failed in steady torsional flow [13]. The calculations reported here, which pinpoint to the better adhesion between the BAMO/AMMO polymer and the wall, suggest that the better adhesion at the wall can delay the onset of wall slip, thus rendering the flow boundary condition more stable. Therefore, the wall–polymer interface again plays an important role in the development of the flow instabilities.

Acknowledgements

We thank Prof German Drazer of CUNY for his input and comments.

References

[1] Aabloo A, Klintenberg M, Thomas JO. Electrochim Acta 2000;45:1425–9.
[2] Tiller AR, Gorella B. Polymer 1994;35(15):3251–9.
[3] Karthigeyan N, Myerson AS. Cryst Growth Des 2001;1(2):131–42.
[4] Akbulut M, Ermler WC, Kalyon DM. Comput Theor Polym Sci 1997;7(2):75–80.
[5] Drazer G, Khusid B, Koplik J, Acrivos A. Phys Fluids 2005;17:102.
[6] Ramamurthy AV. J Rheol 1986;30:337–57.
[7] Chen Y, Kalyon D. J Appl Polym Sci 1993;50:1169–77.
[8] Denn MM. Annu Rev Fluid Mech 2001;33:265–87.
[9] Hill DA. J Rheol 1998;42(3):581–601.
[10] Yarin AL, Graham MD. J Rheol 1998;42(6):1491–504.
[11] Wang SQ, Drda PA. Macromolecules 1996;29(7):2627–32.
[12] Gevgilili H, Kalyon DM. J Rheol 2001;45(2):467–75.
[13] Kalyon DM, Gevgilili H. J Rheol 2003;47(3):683–99.
[14] Cerius^2 Manual, Force field based simulations, MSI, San Diego, CA; 1998.
[15] Mayo SL, Olafson BD, Goddard III WA. J Phys Chem 1990;94:8897.
[16] Berendsen HJC, Postma JPM, van Gunsteren WF, DiNola A, Haak JR. J Chem Phys 1984;81:3684–90.
[17] Gibson HW, Bailey FC. Chem Phys Lett 1977;51(2):352–5.
[18] Ewald PP. Ann Phys 1921;64:253.
[19] Tosi MP. Solid State Phys 1964;16:107.
[20] Billmeyer Jr FW. Textbook of polymer science. 3rd ed. New York: Wiley; 1984 p. 153.
[21] Small PA. J Appl Chem 1953;3:71.